

for worm freezing. Some strains were supplied by the *Caenorhabditis* Genetic Center (CGC), which is supported by the National Institute of Health National Center for Research Resources. This work was supported by grants from the Swiss National Science Foundation, The Ernst Hadorn Foundation and the European Union (FP5 project APOCLEAR) to M.O.H., and by the Max Planck Society and an EU TMR Research Network grant to R.S.

Competing interests statement The authors declare that they have no competing financial interests.

Correspondence and requests for materials should be addressed to M.O.H. (Michael.Hengartner@molbio.unizh.ch).

Phospholipase C γ 1 controls surface expression of TRPC3 through an intermolecular PH domain

Damian B. van Rossum^{1*}, Randen L. Patterson^{4*}, Sumit Sharma¹, Roxanne K. Barrow¹, Michael Kornberg¹, Donald L. Gill⁵ & Solomon H. Snyder^{1,2,3}

¹Departments of Neuroscience, ²Pharmacology and Molecular Science, and ³Psychiatry and Behavioral Sciences, Johns Hopkins University School of Medicine, Baltimore, Maryland 21205, USA

⁴Department of Biology, The Pennsylvania State University, State College, Pennsylvania 16802, USA

⁵Department of Biochemistry and Molecular Biology, University of Maryland School of Medicine, Baltimore, Maryland 21201, USA

* These authors contributed equally to this work

Many ion channels are regulated by lipids^{1–3}, but prominent motifs for lipid binding have not been identified in most ion channels. Recently, we reported that phospholipase C γ 1 (PLC- γ 1) binds to and regulates TRPC3 channels⁴, components

of agonist-induced Ca²⁺ entry into cells. This interaction requires a domain in PLC- γ 1 that includes a partial pleckstrin homology (PH) domain—a consensus lipid-binding and protein-binding sequence^{5,6}. We have developed a gestalt algorithm to detect hitherto ‘invisible’ PH and PH-like domains, and now report that the partial PH domain of PLC- γ 1 interacts with a complementary partial PH-like domain in TRPC3 to elicit lipid binding and cell-surface expression of TRPC3. Our findings imply a far greater abundance of PH domains than previously appreciated, and suggest that intermolecular PH-like domains represent a widespread signalling mode.

An amino-terminal portion of TRPC3 binds to PLC- γ 1 via a sequence of PLC- γ 1 that includes the SH3 domain and the carboxy-terminal half of a split PH domain (PH-c)⁴. To identify the interacting portion of PLC- γ 1 and TRPC3, we conducted a yeast two-hybrid analysis (Fig. 1a). Binding of PLC- γ 1 to TRPC3 requires amino acids 40–46 of TRPC3, with point mutations in this area abolishing binding. TRPC3 binds to PLC- γ 1 PH-c, not the SH3 domain. Moreover, TRPC3 binding seems to be specific for PLC- γ 1 PH-c, as the PH-c domain of AGAP1 does not bind TRPC3, and a single point mutation (F43A) in TRPC3 abolishes β -galactosidase activity in an alternative yeast two-hybrid system (Fig. 1b). *In vitro* protein binding experiments show that PLC- γ 1–TRPC3 interactions are dependent upon amino acids 40–46 of TRPC3 (Fig. 1c, d).

PH domain interactions typically involve full-length PH domains, so the binding of TRPC3 via the PH-c domain of PLC- γ 1 was perplexing. We wondered whether the PH-c domain of PLC- γ 1 might interact with a complementary PH-n domain in TRPC3. Available protein domain search programs (for example, BLAST CDD⁷, Pfam⁸, Prosite⁹ and SMART¹⁰) fail to detect PH domain consensus sequences in TRPC3. However, PH domains that are not recognized by conventional programs exist, exemplified by crystallographically defined PH domains in neurobeachin¹¹, TFIID¹² and RanBP2 (ref. 13). To detect the PH domains in these proteins, we developed a gestalt algorithm to allow greater

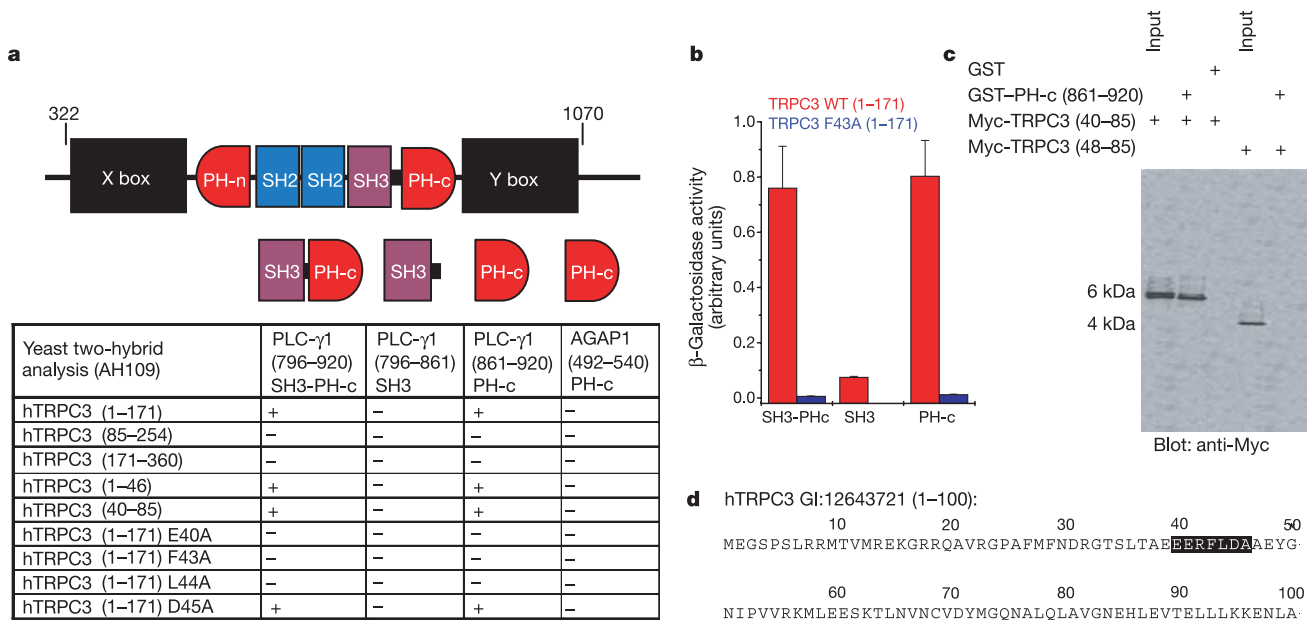


Figure 1 The PLC- γ 1 PH-c domain binds directly to amino acids 40–46 in TRPC3. **a**, Schematic depiction of the catalytic region of PLC- γ . The table depicts the results of yeast two-hybrid screening of rat PLC- γ 1 and human TRPC3 by X- α -Gal blue/white selection in AH109 yeast. **b**, β -Galactosidase activity (1 unit = 1 μ mol of ONPG to o-nitrophenol and D-galactose per min per cell) of pGBKT7-TRPC3 (wild type) or F43A co-transfected with pGADT7-PLC- γ 1 fragments in Y187 yeast. Error bars are standard

error of the mean. **c**, GST pull-down assay of 100 μ g of HEK293 cell lysates expressing Myc-tagged TRPC3 fragments 40–85 or 48–85, incubated with GST alone or GST–PLC- γ PH-c, run on SDS–PAGE and visualized by western blot analysis with anti-Myc. Input lanes are 10 μ g. **d**, hTRPC3 N-terminal amino acids 1–100 with the PLC- γ 1 binding site shaded.

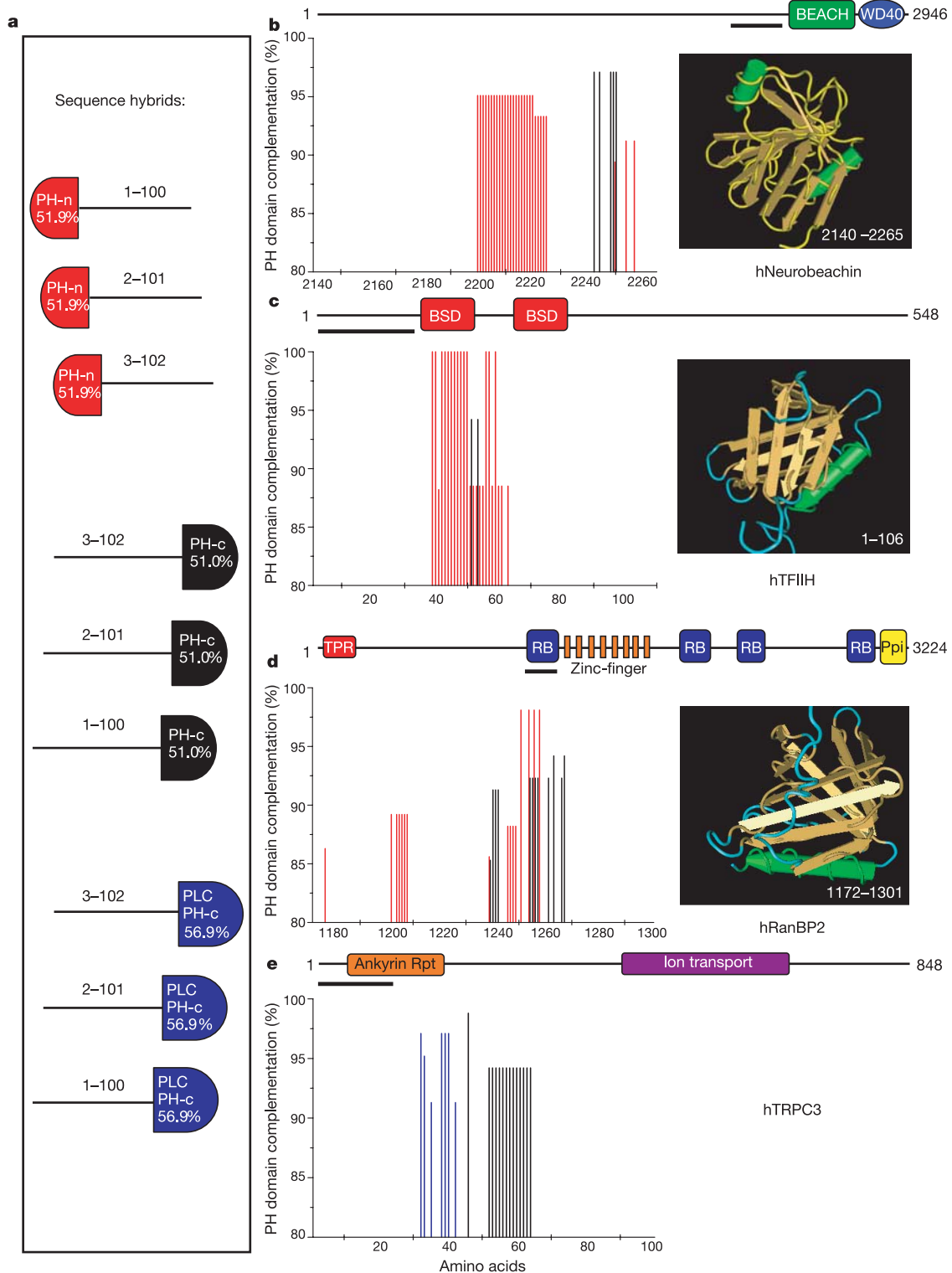


Figure 2 TRPC3 possesses an invisible PH-n domain at the site of PLC- γ 1 PH-c binding. **a**, Schematic depiction of the N-terminal PH consensus hybrids (red), C-terminal PH consensus hybrids (black), or C-terminal PLC- γ 1 PH-c sequence hybrids (blue). **b**, Blast-derived domain architecture of full-length neurobeachin with the region of interest underlined (amino acids 2140–2265; top panel). The left panel shows a graph of PH domain complementation in both N- (red) and C-terminal (black) hybrid directions for each amino acid position. The right panel shows the three-dimensional structure of the

corresponding area, from NCBI's Entrez structure database. **c**, Same as **b** but for hTFIIH (amino acids 1–106). BSD, domain in transcription factors and synapse-associated proteins. **d**, Same as **b** but for hRanBP2 (amino acids 1172–1301). TPR, tetratricopeptide repeats; RB, ran-binding domain; Ppi, peptidyl-prolyl *cis-trans* isomerase. **e**, Same as **b** but for hTRPC3 (amino acids 1–100), with the difference that PLC- γ 1 PH-c sequence hybrids are also plotted.

sequence divergence than conventional methods, which might then be applied to TRPC3. Briefly, by inserting either the N-terminal or C-terminal half of the PH domain consensus into each amino acid position of the target protein we essentially slide a partial PH consensus through the entire coding sequence (Fig. 2a, cartoon). At each sequence-hybrid position we assess PH domain complementation using NCBI Conserved Domain Search⁷ (see Methods). For neurobeachin, in the region containing the PH domain identified by X-ray crystallography (amino acids 2140–2265), we detected up to 95% complementation of a full PH domain whether scanning from the N-terminal (red) or C-terminal direction (black) (Fig. 2b). Similar results are obtained for TFIIH and RanBP2 (amino acids 1–106 and 1172–1301, respectively) (Fig. 2c, d). Screening the entire amino acid sequence of neurobeachin, TFIIH and RanBP2 we detected additional areas of complementation, which might represent other full or partial PH domains (data not shown).

Our studies with neurobeachin, TFIIH and RanBP2 establish the capacity of the algorithm to identify PH domains not predicted by conventional methods. We used this algorithm to seek PH domain sequences in TRPC3 (Fig. 2e). Using consensus PH domain hybrids we detected prominent complementation when scanning from the C-terminal direction (black) (amino acids 50–60) but not from the N-terminal direction. Importantly, scanning TRPC3 with the PH-c sequence of PLC- γ 1 (blue) provides complementation around amino acids 40–48, corresponding exactly to the sequence that binds PLC- γ 1 (see Fig. 1d). For clarity, a raw NCBI Conserved Domain Search derived for a single TRPC3 sequence hybrid is provided (Supplementary Fig. 1). Thus, an intermolecular PH or PH-like domain may exist between PLC- γ 1 PH-c and TRPC3.

Support for TRPC3 possessing a PH-n without a PH-c domain comes from analyses on *smallwing* (*Drosophila* PLC- γ), alpha-1 syntrophin and syngap, where both halves of an ‘invisible’, or split intramolecular PH domain are identifiable (Supplementary Fig. 2).

To assess the functional relevance of the TRPC3–PLC- γ 1 intermolecular PH-like domain, we explored lipid binding, a property of many PH domains^{5,6} (Fig. 3). We generated *in vitro* translated, [³⁵S]methionine-labelled PLC- γ 1 PH-c (861–920), wild-type TRPC3 (1–171) or mutant (F43A) TRPC3 protein, confirmed expression by autoradiography (data not shown), and monitored lipid binding of these proteins alone or in combination on a 15-lipid-strip array. The combination of PLC- γ 1 PH-c and wild-type TRPC3 binds to a pattern of lipids that is distinct from binding observed with PLC- γ 1 PH-c or wild-type TRPC3 alone, most notably phosphatidylinositol-4,5-bisphosphate (PtdIns(4,5)P₂; Fig. 3a, middle panel) and sphingosine-1-phosphate (S1P; data not shown). By contrast, lipid binding by the combination of TRPC3 F43A and PLC- γ 1 PH-c does not differ from PH-c alone, and binding to PtdIns(3,4)P₂ is undetected for all conditions (data not shown). As prototypical PH domains are not established to bind to S1P, binding by the putative TRPC3–PLC- γ 1 intermolecular domain could be due to either a distinct surface/pocket specific to PH-like domains or conformational changes in lipid structure from nitrocellulose immobilization.

To seek physiological relevance we explored TRPC3 Ca²⁺ channel activity *in vivo*. We monitored Fura-2AM-loaded HEK293 cells containing exogenously expressed full-length, Myc-tagged wild-type TRPC3 or the F43A mutant that does not bind PLC- γ 1. Overexpressed TRPC3 can be discriminated from endogenous

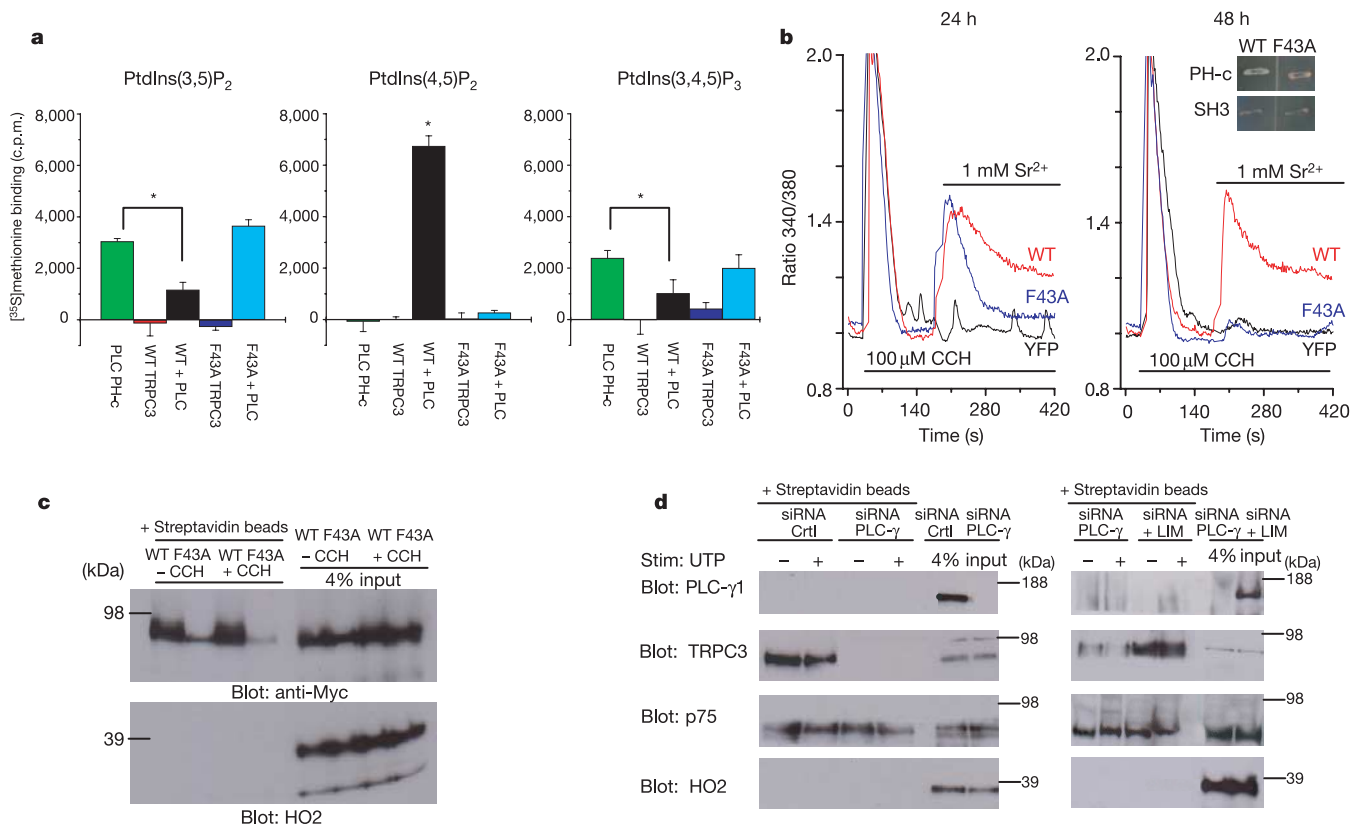


Figure 3 Interaction between PLC- γ 1 PH-c and TRPC3 confers lipid binding and affects membrane expression. **a**, [³⁵S]methionine counts from *in vitro* translated protein(s) incubated over PIP strips. c.p.m., counts per minute. Error bars are standard deviation and *P* value (*) ≤ 0.01 . **b**, Free Ca²⁺ measurements in HEK293 cells transfected for 24 or 48 h with YFP, YFP plus Myc-TRPC3 (wild type) or YFP plus F43A. Ca²⁺ pools were released by carbachol (CCH; first bar) in Ca²⁺-free medium followed by replacement with

Sr²⁺ (second bar). The inset shows yeast growth on selective media. **c**, Western blot of biotinylated HEK293 cells transfected with wild-type TRPC3 or the F43A mutant for 48 h, treated with or without CCH (100 μ M). Input lanes 20 μ g. **d**, Western blot of biotinylated rat PC12 cells transfected with scrambled siRNA or rPLC- γ 1 siRNA with or without hPLC- γ 1 lipase-inactive mutant (LIM) and UTP (100 μ M). Input lanes 20 μ g.

TRPC channels by replacing Ca^{2+} (1 mM) in the bathing medium with Sr^{2+} (1 mM), the flux of which selectively uses the over-expressed channels^{4,14}. At 24 h posttransfection, TRPC3 channel activity is the same for wild type and F43A (Fig. 3b, left). By contrast, at 48 h mutant channel activity is abolished, whereas robust wild-type channel activity persists (Fig. 3b, right).

As the F43A channel cannot bind PLC- γ 1, its channel gating is independent of PLC- γ 1. Therefore, we wondered how PLC- γ 1 was regulating TRPC3 activation through G_q -coupled muscarinic receptor stimulation. One possibility is protein stability; however, we detected little difference in expression between the wild-type and F43A TRPC3 channel at 48 h (Fig. 3c). The normal channel activity of the F43A mutant at 24 h indicates that it can localize to the plasma membrane. This finding, combined with the normal total level of mutant TRPC3 at 48 h, implies a defect in cell-surface expression of the channel at 48 h. Accordingly, we examined the cell-surface disposition of overexpressed wild-type and mutant channels at 48 h using cell-surface biotinylation (Fig. 3c). Whereas wild-type TRPC3 is expressed in the plasma membrane at 48 h, levels of the mutant channel are significantly reduced, with total protein levels being unaffected. We ascertained whether short interfering (si)RNA-induced depletion of PLC- γ 1 would influence cell-surface

levels of endogenous TRPC3 (Fig. 3d). Depletion of PLC- γ 1 reduces endogenous TRPC3 in the plasma membrane whereas a scrambled siRNA control does not. Regulation of Ca^{2+} entry by PLC- γ 1 is independent of its lipase function⁴. Rescued expression of human PLC- γ 1 lipase-inactive mutant restores plasma membrane expression of endogenous TRPC3 in the siRNA preparation (Fig. 3d, right).

These findings imply that TRPC3–PLC- γ 1 intermolecular PH-like domain formation regulates surface expression of TRPC3. However, these conclusions are based solely upon the use of the F43A mutant. From this alone one cannot conclude that formation of the predicted PH-like domain is responsible for the observed $\text{PtdIns}(4,5)\text{P}_2$ binding. Similarly, one cannot conclude that $\text{PtdIns}(4,5)\text{P}_2$ binding is important for function, as the F43A mutation disrupts the TRPC3–PLC- γ 1 complex. To investigate both questions requires the construction of a TRPC3 mutant that retains the ability to interact with PLC- γ 1 and generate the PH-like domain, but cannot bind $\text{PtdIns}(4,5)\text{P}_2$. TRPC3 contains eight conserved arginine or lysine residues in the predicted B1–B3 loop (amino acids 1–39, see Fig. 1d). Taking advantage of PLC- γ 1 PH-c complementation within wild-type TRPC3 at seven discrete points (blue lines in Fig. 2e), we discriminated which residues may be

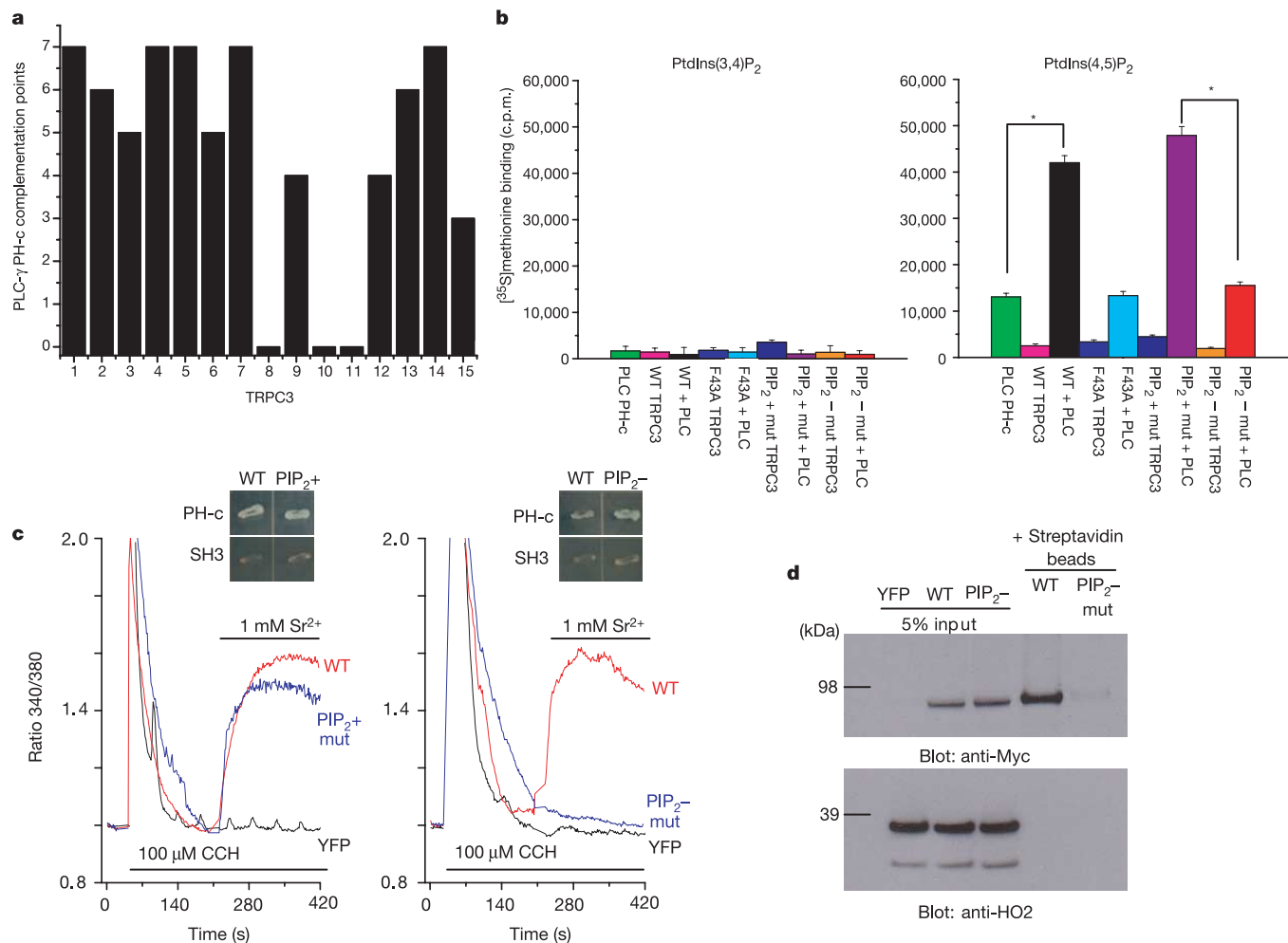


Figure 4 Intermolecular PH-like domain formation controls the surface expression of TRPC3. **a**, *In silico* scanning alanine mutagenesis predicts TRPC3 mutants retaining (PIP₂⁺mut) and lacking (PIP₂⁻mut) lipid binding. Lanes: 1, WT; 2, R8A; 3, R9A; 4, R8A/R9A (PIP₂⁺mut); 5, R14A; 6, K16A; 7, R18A; 8, R19A; 9, R14A/K16A; 10, R14A/K16A/R18A; 11, R14A/K16A/R18A/R19A (PIP₂⁻mut); 12, R23A; 13, R32A; 14, R42A; 15, R23A/R32A/R42A. **b**, [³⁵S]methionine counts from *in vitro* translated protein(s) incubated

over lipid-conjugated agarose beads. Error bars are s.d. and *P* value (*) ≤ 0.01. **c**, Free Ca²⁺ measurements in HEK293 cells transfected for 24 h with YFP alone or YFP plus Myc-TRPC3 (wild type), PIP₂⁺mut, or PIP₂⁻mut. Ca²⁺ pools were released in cells by CCH (first bar) followed by replacement with Sr²⁺ medium (second bar). The insets show yeast growth on selective media. **d**, Western blot of biotinylated HEK293 cells transfected with YFP alone, Myc-tagged TRPC3 (wild type) or PIP₂⁻mut for 24 h. Input lanes 20 μg.

involved in PtdIns(4,5)P₂ binding by conducting *in silico* scanning alanine mutagenesis (Fig. 4a). PH domain complementation by wild-type TRPC3 and R8A/R9A (PIP₂+mut) are similar; however, within the TRPC3 mutant R14A/K16A/R18A/R19A (PIP₂-mut) complementation is abolished (Fig. 4a). For both TRPC3 mutants (1–171), binding to PLC-γ1 PH-c (861–940) was confirmed by yeast two-hybrid analysis (Fig. 4c, inset).

We used PIP₂-conjugated agarose beads as an independent method to assay lipid binding. Specificity of binding was compared between PtdIns(3,4)P₂ and PtdIns(4,5)P₂, as these lipids have similar charge distribution. We generated *in vitro* translated, [³⁵S]methionine-labelled PLC-γ1 PH-c (861–940), wild-type TRPC3 (1–171), F43A, PIP₂+mut and PIP₂-mut, and confirmed expression by autoradiography (data not shown). We monitored lipid binding of these proteins alone or in combination. The combination of PLC-γ1 PH-c and wild-type TRPC3 or PIP₂+mut binds to PtdIns(4,5)P₂, with little to no PtdIns(3,4)P₂ binding (Fig. 4b). By contrast, the combination of PLC-γ1 PH-c and TRPC3 mutants F43A or PIP₂-mut does not differ compared with PH-c alone. This establishes a lipid-binding function for the TRPC3–PLC-γ1 intermolecular PH-like domain, and is the first direct evidence of lipid binding within the TRP superfamily.

To ascertain whether lipid binding modulates surface expression we monitored Fura-2AM-loaded HEK293 cells containing exogenously expressed full-length, Myc-tagged wild-type TRPC3, PIP₂+mut, or PIP₂-mut. At 24 h post-transfection, channel activity is the same for wild-type TRPC3 and PIP₂+mut (Fig. 4c, left). By contrast, at 24 h the activity of the TRPC3 PIP₂-mut channel is abolished (Fig. 4c, right). We examined the cell-surface disposition of overexpressed wild-type and PIP₂-mut channels at 24 h using cell-surface biotinylation (Fig. 4d). Whereas wild-type TRPC3 is expressed in the plasma membrane, PIP₂-mut channel levels are markedly reduced in the plasma membrane, with total protein levels being unaffected.

We wondered whether other instances of lipid binding might involve hitherto unrecognized PH-like domains. One study² identified a novel consensus sequence in TRPV1 and certain potassium channels that mediate PIP₂ modulation. Our algorithm for PH-like domains reveals complementation in the exact area (amino acids 780–819) known to mediate PIP₂ regulation of TRPV1. Furthermore, in yeast two-hybrid analysis, PLC-γ1 PH-c domain binds to rat (r)TRPV1 in a similar area to that of TRPC3 (peptide EEVQL versus EERFL, respectively), suggesting functional symmetry between these two channels (Supplementary Fig. 3).

Our findings provide a molecular mechanism for the regulation of agonist-induced Ca²⁺ entry by PLC-γ1 (ref. 4). Specifically, PLC-γ1 forms an intermolecular PH-like domain with TRPC3, regulating lipid binding and surface expression of TRPC3. Evidence includes: (1) an algorithm that identifies ‘invisible’ PH and PH-like domains; (2) elucidation of such a domain in TRPC3, which, with PLC-γ1 PH-c, binds to PtdIns(4,5)P₂ *in vitro*; (3) elimination of lipid binding by selective mutation of TRPC3 in either its PLC-γ1 PH-c binding site or its predicted B1–B3 loop; (4) abolition of TRPC3 activity by these selective mutations; and (5) blockade of cell-surface expression of endogenous TRPC3 by siRNA-induced depletion of PLC-γ1.

Our gestalt algorithm for identifying invisible PH domains can reveal previously unrecognized PH domains, exemplified by its detection of PH domains in neurobeachin, TFIH and RanBP2, which could only be realized through X-ray crystallography. Furthermore, this algorithm, a partial consensus sequence that slides across a protein’s amino acid sequence, may identify other hidden domains as well. □

Methods

Yeast two-hybrid analysis

Experiments were performed with the Matchmaker 3 yeast two-hybrid system (Clontech),

following the manufacturer’s instructions, with pGBK7-BD-TRPC3 fragments and pGADT7-AD-PLC-γ1 or AGAP fragments (where AD and BD indicate β-galactosidase-activating domain and β-binding domain, respectively). Human (h)TRPC3 mutations were introduced using the QuikChange site-directed mutagenesis kit (Stratagene) and confirmed by sequencing.

GST pull down

Cell lysis buffer (150 mM NaCl, 50 mM Tris, pH 7.8, 1% Triton X-100, 1 mM EDTA) was added to 100 μg of Myc-TRPC3 40–85- or 46–85-expressing HEK293 whole-cell lysates (total volume 500 μl). GST–Sepharose beads and purified GST–PLC-γ1 PH-c or GST were added, incubated on a rotator for 1 h at 4 °C, washed three times with lysis buffer and quenched with 20 μl of SDS sample buffer. Co-precipitates were resolved by SDS–PAGE and analysed by western blot analysis (input lanes 10 μg).

Domain alignments

We generated serial hybrid sequences comprised of a target sequence (for example, human neurobeachin GI:21536252, hTFIIH GI:416727, hRanBP2 GI:6382079 or hTRPC3 GI:12643721) and a partial PH domain ‘donor’ sequence inserted at each target amino acid position either N-terminally or C-terminally. PH-n front consensus, VIKEGWLLKSSGKSSWKKRYFVLFNGV LLYYKSKKKSSSKPKGSIPLSGCT; PH-c back consensus, GCTVREAPDSDSKKNCFEIVTPDRKTLQLQAEEEREVEWVEALR KAIKAI; and rPLC-γ1 (GI:6981370) PH-c sequence (865–930), NSPLGDLRLGVLDV PACQAIIRPEGGKNNRFLVF SISMPVAQWLSLDAVADSQELQDWWKIREVA.

Domain searches were performed using NCBI Conserved Domain Database (<http://www.ncbi.nlm.nih.gov/Structure/cdd/wrpsb.cgi>) on overlapping, 150-amino-acid hybrid fragments (settings: search database CDDv2.00-11382 PSSMS, expect 0.01, no filter, search mode multiple hits 1-pass). Significant PH domain complementation was monitored as a change in the SMART or PFAM conserved domain length greater than or equal to 85% (because scores for neurobeachin, TFIH and RanBP2 did not fall below this cutoff) and was plotted on the y axis at the respective target amino acid hybrid point.

In vitro translation

In vitro translation of BD-TRPC3 and AD-PLC-γ vectors was performed using Promegas TNT quick-coupled transcription/translation systems following the manufacturer’s instructions.

Lipid binding

PIP strips (Echelon P-6001) cut into individual spots were blocked in Tris-buffered saline with 0.1% Tween and 3% fatty-acid-free bovine serum albumin (Sigma) (TBST-3% BSA) for 1 h. Each spot was incubated for 3 h at room temperature with 500 μl of TBST-3% BSA plus 10 μM of the *in vitro* translated protein(s) of interest, washed six times in 1 ml of TBST-3% BSA, dissolved in 6 ml of scintillation fluid overnight and counted. The blank spot was used to subtract background from the remainder of the samples. A total of 20 μl bed volume of PIP₂ beads was equilibrated in 1 ml of TBS with 0.5% Tween overnight. Equilibration buffer was removed and replaced with 200 μl of 0.5% TBST containing 10 μM of the appropriate [³⁵S]methionine-labelled construct(s) and incubated for 2 h at room temperature, washed ten times in 1 ml 0.5% TBST, transferred to scintillation fluid and counted. Background counts obtained from PIP₂ beads incubated with mock-translated rabbit reticulocyte lysate containing empty vector and [³⁵S]methionine were subtracted from all samples. In control experiments (data not shown), [³⁵S]methionine-labelled β-galactosidase-activating domain (AD), -binding domain (BD), or AD plus BD failed to bind to any lipid spot or bead. Each experiment was performed a minimum of three times, and the data expressed in the bar graphs are averages of triplicates obtained from one experiment. Error bars represent the standard deviation from one experiment and all significance is ≤0.01.

Calcium measurements

Ca²⁺ measurements were as described¹⁴. All traces are averages from multiple (30–50) cells and are representative of at least three individual experiments. Fluorescence emission at 505 nm was monitored with excitation at 340 and 380 nm; Ca²⁺ measurements are shown as 340/380-nm ratios obtained from averages of single cells.

TRPC3 antibody

Rabbit polyclonal antiserum against TRPC3 was generated by injecting New Zealand white male rabbits with the peptide MREKGRRQAVRGPAFMFNDRC coupled to keyhole limpet haemocyanin (Pierce Biotechnology). Initial injection was with complete Freund’s adjuvant, and boost injections at days 14, 21 and 49 were with incomplete Freund’s adjuvant. Rabbit injections, bleeds and housing were performed by Cocalico Biologicals. Antibodies were affinity purified using the antibody peptide coupled to the Pierce Biotechnology Ultralink iodoacetyl column, as per the manufacturer’s instructions.

Cell-surface biotinylation

HEK293 cells were transfected with Myc-TRPC3 constructs for 24 or 48 h, and PC12 cells with either scrambled, PLC-γ1 siRNA⁴, or siRNA plus Flag-tagged, lipase-inactive human PLC-γ1 for 48 h. Cells were washed three times in 10 ml ice-cold PBS pH 8, and incubated in 6 ml of 1 mM Sulpho-NHS-LC-biotin (Pierce) in PBS pH 8 for 3 h. Cells were quenched with 10 ml of PBS pH 8, 10 mM Tris and 100 mM glycine for 10 min, washed twice in 10 ml PBS pH 8, lysed (500 μl RIPA buffer) and the protein assay performed. A total of 500 μg of cell lysate was dissolved in 500 μl of RIPA buffer plus 25 μl bed volume of streptavidin-agarose beads, and rocked overnight. Beads were washed ten times in 1 ml RIPA buffer, boiled in 30 μl sample buffer, and analysed by SDS–PAGE and western blot analysis. Polyclonal anti-HO2 antibody¹⁵ served as a negative control for surface labelling, and

p75 (a surface receptor) served as a cell-surface control for siRNA-induced PLC- γ 1 depletion.

Reagents

Enhanced yellow fluorescent protein (YFP) vector and Lipofectamine were from Clontech; anti-Myc, [³⁵S]methionine, carbachol, ONPG and GST–Sepharose were from Sigma; Fura-2/acetoxymethyl ester was from Molecular Probes. siRNA duplexes were from Dharmacon Research. Anti-p75 antibody was from Upstate.

Received 18 August; accepted 17 December 2004; doi:10.1038/nature03340.

1. Runnels, L. W., Yue, L. & Clapham, D. E. The TRPM7 channel is inactivated by PIP(2) hydrolysis. *Nature Cell Biol.* **4**, 329–336 (2002).
2. Prescott, E. D. & Julius, D. A modular PIP2 binding site as a determinant of capsaicin receptor sensitivity. *Science* **300**, 1284–1288 (2003).
3. Suh, B. C. & Hille, B. Recovery from muscarinic modulation of M current channels requires phosphatidylinositol 4,5-bisphosphate synthesis. *Neuron* **35**, 507–520 (2002).
4. Patterson, R. L. *et al.* Phospholipase C- γ is required for agonist-induced Ca²⁺ entry. *Cell* **111**, 529–541 (2002).
5. DiNitto, J. P., Cronin, T. C. & Lambright, D.G. Membrane recognition and targeting by lipid-binding domains. *Sci. STKE*. re16 (2003).
6. Rebecchi, M. J. & Scarlata, S. Pleckstrin homology domains: a common fold with diverse functions. *Annu. Rev. Biophys. Biomol. Struct.* **27**, 503–528 (1998).
7. Marchler-Bauer, A. *et al.* CDD: a curated Entrez database of conserved domain alignments. *Nucleic Acids Res.* **31**, 383–387 (2003).
8. Bateman, A. *et al.* The Pfam protein families database. *Nucleic Acids Res.* **32**, D138–D141 (2004).
9. Gattiker, A., Gasteiger, E. & Bairoch, A. ScanProsite: a reference implementation of a PROSITE scanning tool. *Appl. Bioinform.* **1**, 107–108 (2002).
10. Letunic, I. *et al.* SMART 4.0: towards genomic data integration. *Nucleic Acids Res.* **32**, D142–D144 (2004).
11. Jogl, G. *et al.* Crystal structure of the BEACH domain reveals an unusual fold and extensive association with a novel PH domain. *EMBO J.* **21**, 4785–4795 (2002).
12. Gervais, V. *et al.* TFIIH contains a PH domain involved in DNA nucleotide excision repair. *Nature Struct. Mol. Biol.* **11**, 616–622 (2004).
13. Vetter, I. R., Nowak, C., Nishimoto, T., Kuhlmann, J. & Wittinghofer, A. Structure of a Ran-binding domain complexed with Ran bound to a GTP analogue: implications for nuclear transport. *Nature* **398**, 39–46 (1999).
14. Ma, H. T. *et al.* Requirement of the inositol trisphosphate receptor for activation of store-operated Ca²⁺ channels. *Science* **287**, 1647–1651 (2000).
15. Baranano, D. E. *et al.* A mammalian iron ATPase induced by iron. *J. Biol. Chem.* **275**, 15166–15173 (2000).

Supplementary Information accompanies the paper on www.nature.com/nature.

Acknowledgements We thank D. Boehning, G. Caraveo, J. Kendall, A. Resnick and R. E. Rothe for discussion; P.-G. Suh for the gift of the PLC- γ 1 antibody; and B. VanRossum for graphics. This research was supported by US Public Health Service Grants and a Research Scientist Award (to S.H.S.), a National Institutes of Health Grant (to D.L.G.), and National Research Service Awards (to R.L.P.).

Competing interests statement The authors declare that they have no competing financial interests.

Correspondence and requests for materials should be addressed to S.H.S. (ssnyder@jhmi.edu).

Cyclin specificity in the phosphorylation of cyclin-dependent kinase substrates

Mart Loog & David O. Morgan

Department of Physiology, University of California, San Francisco, California 94143-2200, USA

Cell-cycle events are controlled by cyclin-dependent kinases (CDKs), whose periodic activation is driven by cyclins. Different cyclins promote distinct cell-cycle events, but the molecular basis for these differences remains unclear^{1,2}. Here we compare the specificity of two budding yeast cyclins, the S-phase cyclin Clb5 and the M-phase cyclin Clb2, in the phosphorylation of 150 Cdk1 (Cdc28) substrates. About 24% of these proteins were phosphorylated more efficiently by Clb5–Cdk1 than Clb2–Cdk1.

The Clb5-specific targets include several proteins (Sld2, Cdc6, Orc6, Mcm3 and Cdh1) involved in early S-phase events. Clb5 specificity depended on an interaction between a hydrophobic patch in Clb5 and a short sequence in the substrate (the RXL or Cy motif). Phosphorylation of Clb5-specific targets during S phase was reduced by replacing Clb5 with Clb2 or by mutating the substrate RXL motif, confirming the importance of Clb5 specificity *in vivo*. Although we did not identify any highly Clb2-specific substrates, we found that Clb2–Cdk1 possessed higher intrinsic kinase activity than Clb5–Cdk1, enabling efficient phosphorylation of a broad range of mitotic Cdk1 targets. Thus, Clb5 and Clb2 use distinct mechanisms to enhance the phosphorylation of S-phase and M-phase substrates.

A long-standing question in cell-cycle control is how different cyclins drive the distinct events of S phase and M phase^{1,2}. One model, termed the quantitative model of cyclin function, suggests that S phase is triggered by low levels of cyclin–CDK activity and M phase is initiated at higher levels of activity^{3,4}. According to this model, apparent differences in cyclin function are due primarily to differences in their timing and levels of expression. In contrast, the qualitative model proposes that different cyclins possess different intrinsic functional capacities, perhaps because they modulate the substrate specificity of the associated CDK or alter its subcellular location^{1,5}. Studies in budding yeast, for example, argue that the S-phase cyclin Clb5 possesses higher intrinsic S-phase-promoting activity than the M-phase cyclin Clb2 (refs 6, 7). Biochemical studies with mammalian cyclins have demonstrated cyclin specificity in the phosphorylation of a small number of substrates: for example, mammalian cyclin-A–CDK, but not cyclin-B–CDK, phosphorylates the pRb-related protein p107 (ref. 8). However, few cyclin-specific substrates have been identified in any species, and the general importance of cyclins in CDK substrate specificity remains unclear.

To assess the global importance of cyclin specificity in cell-cycle control, we measured the phosphorylation of a large number of Cdk1 substrates by S-phase and M-phase cyclin–CDK complexes. We recently identified 181 budding yeast Cdk1 substrates⁹, and in the present study we measured the kinase activities of Clb5–Cdk1 and Clb2–Cdk1 towards 150 of these proteins (obtained from proteomic libraries; see Methods). To prevent background phosphorylation by contaminating protein kinases in the reactions, we used a mutant form of Cdk1, Cdk1-as1, that contains an enlarged ATP-binding site. Purified Clb5–Cdk1-as1 or Clb2–Cdk1-as1 complexes were incubated with the test substrate and the bulky ATP analogue [γ -³²P]N⁶-(benzyl)ATP, which only the mutant Cdk1-as1 enzyme can use⁹. Reactions were performed with amounts of Clb5–Cdk1-as1 and Clb2–Cdk1-as1 that possessed equal activities toward the non-specific substrate histone H1 (Fig. 1a). Phosphate incorporation was then divided by the amount of substrate protein, and the logarithm of this ratio was designated as the substrate P-score, as described previously⁹. All reactions were performed at very low substrate concentrations (presumably well below K_m); thus, differences in P-scores between the two kinases provide a reasonable estimate of relative k_{cat}/K_m values, where K_{cat} is catalytic constant and K_m is Michaelis constant.

All substrate P-scores for the two kinases are plotted in Fig. 1b. These data suggest that, on a histone H1-normalized scale, most of the substrates – about 110 of the 150 – are equally good substrates for Clb5–Cdk1 and Clb2–Cdk1, because they exhibit 2.5-fold or less specificity for either kinase and fall in the middle diagonal region of the plot. Most of the remaining substrates, falling to the right of the diagonal, are specific for Clb5. Among these were 14 substrates with specificity for Clb5 ranging from 10-fold to 800-fold, whereas 22 proteins displayed specificity of between 2.5-fold and 10-fold (note that the scale on this plot is logarithmic). The top Clb5-specific substrates included several proteins involved in DNA replication (Orc6, Orc2, Mcm3, Cdc6 and Sld2), spindle pole body function